

Contents

1	Summary	1
2	Problem definition and background	2
2.1	Theoretical background	2
2.2	Reference solution	2
2.2.1	Sauer method	3
3	Design of Experiment	5
4	Computational model	6
4.1	Problem geometry and setup	6
4.2	Mesh generation and description	7
4.2.1	Euler case	7
4.2.2	RANS case	7
4.3	Numerical schemes	8
5	Results	10
5.1	Euler case	10
5.1.1	Grid convergence	10
5.1.2	Comparison between ROE and JST scheme	11
5.1.3	Comparison between 1st and 2nd order solutions	12
5.2	RANS case	14
5.2.1	Grid convergence	14
5.2.2	Comparison between SA and SST turbulence model	16
5.2.3	Comparison between 1st and 2nd order scheme	16
5.3	Comparison between Euler, RANS and Quasi 1D	17
5.4	Comparison with experimental data	19
5.5	Sauer method	20
6	Conclusions	21

1. Summary Abstract: goal of the work, strategy, main results

This report presents the analysis of the flow inside a converging-diverging nozzle geometry which is an useful case for investigating compressible flows whose thermodynamic behavior cannot be properly described by the simple ideal-gas law. In particular siloxane MDM (octamethyltrisiloxane, $C_8H_{24}O_2Si_3$), a high molecular complexity organic compound, is used for our simulations. Acting on the value of the pressure at the outlet we are able to compare different work conditions of the nozzle. The problem will be tackled both with Euler and RANS equations and the results will be also compared with the quasi 1D theory.

2. Problem definition and background

2.1 Theoretical background Keep it short and focused.

The flow in a nozzle can be described using *Quasi 1d Theory* in which all properties are assumed to vary only along the axis of the duct/streamtube, which is taken to be the x direction. The hypothesis of this theory are:

- Steady, inviscid, adiabatic flow
- Quasi-one-dimensional flow: if the variation of area $A = A(x)$ of the duct is gradual, it is often convenient and sufficiently accurate to neglect the y and z flow variations, and to assume that the flow properties are function of x only. Therefore:

$$P = P(x) \quad \rho = \rho(x) \quad T = T(x) \quad u = u(x) \quad A = A(x)$$

Enforcing conservation equation and the additional hypothesis of *isentropic flow* we are able to write relations that link the variation of area with the velocity and then the velocity with variation of ρ , P , c , M . Moreover, for a polytropic ideal gas we are able to obtain for example:

$$\frac{A}{A_0} = \frac{M_0}{M} \left[\frac{1 + \frac{\gamma-1}{2} M^2}{1 + \frac{\gamma-1}{2} M_0^2} \right]^{\frac{\gamma+1}{2(\gamma-1)}} \quad (2.1)$$

Where A_0 and M_0 are respectively the area and the Mach at a reference point. Since the geometry of the nozzle is set, it is easy to find the value of Mach for each section. If the flow is subsonic, an increasing section will lead to a decreasing velocity, while a decreasing section to an increasing velocity. On the other hand, if the flow is supersonic, an increasing section will lead to an increasing velocity and the opposite will occur if the area decrease. Moreover, under these assumptions we can use relations that for an ideal polytropic gas link total and static quantities (T, P, ρ) with the local Mach number.

$$\frac{T^t}{T} = \left[1 + \frac{\gamma-1}{2} M^2 \right] \quad \frac{P^t}{P} = \left[1 + \frac{\gamma-1}{2} M^2 \right]^{\frac{\gamma}{\gamma-1}} \quad \frac{\rho^t}{\rho} = \left[1 + \frac{\gamma-1}{2} M^2 \right]^{\frac{1}{\gamma-1}}$$

2.2 Reference solution

During the report will be analyzed three different work conditions depending on the value of the outlet pressure. Applying the *Quasi 1D* theory, we are able to describe the evolution of flow properties. In case in which a shock wave occurs we should use Rankine-Hugoniot relations in order to link flow properties before and after the shock wave. For each work condition we have a different behaviour that is described below, where the value of pressure is the one used in our simulations for each case:

- Shock wave in the divergent ($P_{out} = 650000 Pa$): flow velocity increases in the convergent reaching sonic Mach in the throat, after that, in the divergent it keeps increasing until it reaches the shock wave. The shock causes the passage from a supersonic Mach to a subsonic one that decreases a bit until it reaches the outlet of the nozzle. The shock wave is needed in order to accomplish the value of outlet pressure imposed in the boundary conditions. On the other hand pressure decreases both in the convergent and in the divergent until the shock is reached and there we have a sudden jump that leads to an increase of the pressure. Then, this value keeps increasing till the end of the nozzle. In order to reach this result we consider isentropic flow up to the shock wave, we use Rankine-Hugoniot relations to solve the shock wave and then, after the shock, we consider again isentropic conditions.
- Design condition ($P_{out} = 253340 Pa$): the value of Mach keeps increasing while the pressure decreases until it reaches the outlet boundary value at the end of the nozzle. In this condition the shock wave is stuck in the throat and there we reach Mach equal to one. In this case we have a completely isentropic expansion and an adapted flow.
- Subsonic condition ($P_{out} = 800000 Pa$): the Mach remains always under the sonic value. Velocity increases in the divergent until the throat and the start decreasing, while the pressure has the opposite behaviour. Of course, no shock wave occurs in this case.

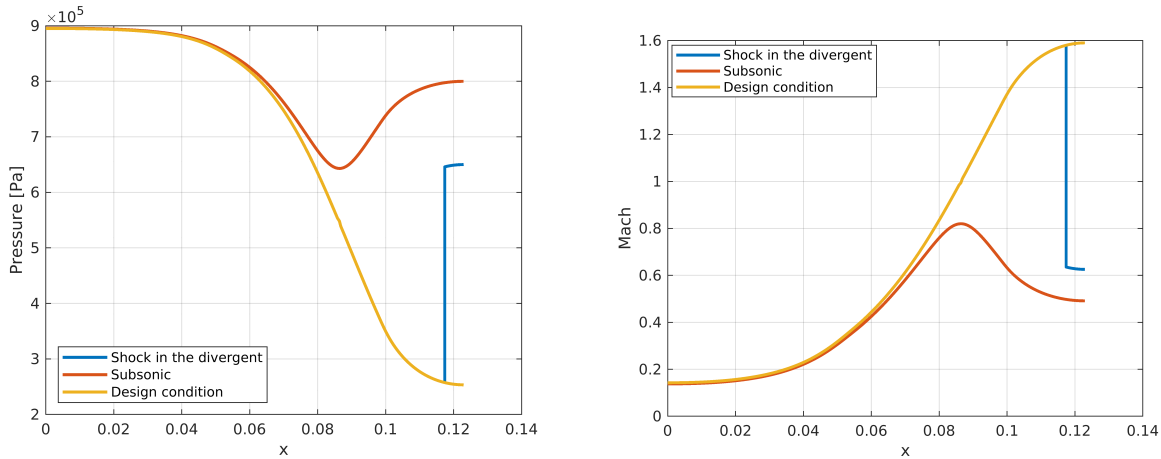


Figure 2.1: Solution computed with Quasi 1D theory for the three analyzed cases

2.2.1 Sauer method

Another theory that we will use in order to check our results is the *Sauer method*. This method stands under the following hypothesis:

- continuous flow quantities;
- homoentalpic and homoentropic flow;
- the function that describes the nozzle $y = \eta(x)$, in the throat must be: $\eta(x_t) \in C^2$

If these hypothesis are verified we can use this method to find the sonic line where $M = 1$:

$$x = -\frac{\gamma + 1}{2} \alpha y^2 \quad (2.2)$$

where the parameter α and the origin of the reference system ε can be computed as follow:

$$\alpha = \sqrt{\frac{1}{\gamma + 1} \frac{1}{r_t y_t}} \quad \varepsilon = -\frac{\gamma + 1}{6} \alpha y_t^2$$

This means that we are able to define the sonic line shape knowing the values of the curvature radius r_t and the throat height y_t . Usually, the Sauer method can be considered correct only if these parameters satisfy:

$$r_t/y_t > 2$$

3. Design of Experiment

We develop our analysis using both for the Euler and the RANS case and the main step are presented below:

- **Euler case:**

1. **Mesh convergence:** the first step is to reach mesh convergence and this is done using a ROE scheme and refining the mesh both for the first and the second order (activating the *MUSCL_FLOW* option). In this way we are able to reach a mesh that allows us to present results which are independent from further refinements of the grid both for the first and the second order. Mesh convergence will be presented for the most troublesome condition, meaning the case for which a shock wave is generated in the divergent part of the nozzle.
2. **Comparison between the results** obtained with a second order ROE scheme and a second order JST scheme. Both are obtained with the *MUSCL_FLOW* option on.
3. **Comparison between different work conditions of the nozzle**, obtained acting on the value of the pressure at the outlet. In particular we consider three possibilities: subsonic nozzle, design condition (sonic Mach at the throat), shock wave in the divergent.

- **RANS case:**

1. **Mesh convergence:** also in this case the first step consists in redoing the convergence of the grid since the equations and mesh type are different from before. This is done both for the first order and second order ROE scheme, taking into account the case for which a shock wave is generated in the divergent part of the nozzle. Moreover we will also show that grid convergence is still guaranteed if we consider a total subsonic case or the design condition.
2. Comparison between the results obtained **with the SA and the SST turbulence model**
3. Comparison between first and second order ROE scheme on the solution referred to the case with a shock wave in the divergent.
4. **Comparison between the numerical results and the experimental data** reported by *Spinelli A., Cammi G., Gallarini S., Zocca M., Cozzi F., Gaetani P., Dossena V., Guardone A. Experimental evidence of non ideal compressible effects in expanding flow of a high molecular complexity vapor, Experiments in Fluids (2018) 59:126.*

Eventually a comparison between Euler and RANS cases will be carried out taking into account also the theoretical solution of the *Quasi 1D Theory*.

4. Computational model

4.1 Problem geometry and setup

The geometry of the nozzle considered for this report reproduces the test section of the Test-Rig for Organic Vapors (TROVA), a wind tunnel for non-ideal compressible flows at CREA Lab of Politecnico di Milano. The total length of the nozzle is $0.123m$, with an inlet height of $0.036m$ and a throat height of $0.0084m$. The following figure shows the adopted geometry and an indication of the boundary conditions.

Geometry and domain information

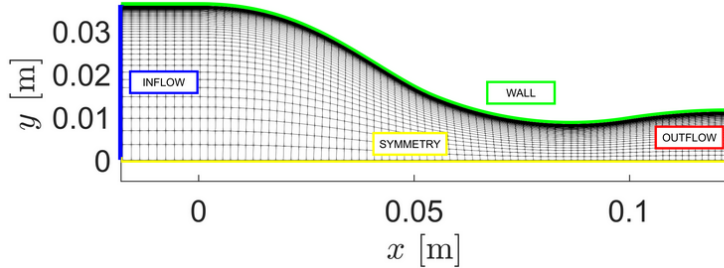


Figure 4.1: Nozzle geometry and boundary condition markers

The Navier-Stokes adiabatic wall condition is imposed on the WALL boundary for the RANS case while in the Euler case it is simply a no-penetration constraint. The symmetry boundary condition is used at the SYMMETRY boundary: the symmetry condition mirrors the flow about the x axis, thus allowing to reduce the size of the mesh and the computational cost. At the outlet we impose the value of the static pressure and this will change depending on the analysed case: subsonic nozzle, design condition(sonic Mach at the throat), shock wave in the divergent. At the INLET we impose the total conditions of the flow that is directed only in x-direction:

- Inlet Stagnation Temperature = $542.13K$
- Inlet Stagnation Pressure = $904388Pa$
- Inlet Flow Direction, unit vector $(x,y,z) = (1.0, 0.0, 0.0)$

In design conditions, the total to exhaust pressure ratio of the nozzle is 3.125, which gives a supersonic outflow at Mach number 1.5. For simulations a non ideal flow, Siloxane MDM (*octamethyltrisiloxane*, $C_8H_{24}O_2Si_3$), a high molecular complexity organic compound, is used.

4.2 Mesh generation and description

4.2.1 Euler case

The study to achieve grid convergence leads us to the generation of different unstructured meshes made with triangular elements. The generation of the mesh requires the setting of the spacing h at the airfoil surface. Moreover we have to impose also the type of algorithm that in this case will be the Adaptive algorithm. In order to generate the `.geo` file from a set of data that represents the geometry of the nozzle we use the `printGeo` tool. This requires us the setting of some parameters:

- Inlet spacing = 5 , meaning that the element size at the inlet is 5 times the one at the throat of the nozzle.
- Outlet spacing = 1 , meaning that the element size at the outlet is equal to the size of the one at the throat.

These values are used also to generate the mesh for the RANS case and the following table summarize the other imposed parameters.

	h	Elements
Mesh 1	0.0005	5858
Mesh 2	0.0003	16360
Mesh 3	0.0002	37578
Mesh 4	0.0001	149203
Mesh 5	0.00008	231410

Mesh information:

- type of grid
- # nodes or elements,
- grid spacing

4.2.2 RANS case

In this case we are interested in resolving also the boundary layer at nozzle wall. For this reason we generate an hybrid mesh which is structured near to the wall and becomes unstructured in the rest of the domain inside the nozzle. The `.geo` file is created as explained for the Euler case and after that we have to define also the parameters for the structured part near the wall and for this reason we need to set: the expansion ratio, the dimension of the first element at the wall, the thickness of this layer. In particular in our meshes we will one of the two following set of parameters for the structured part of the boundary layer:

- Structured part *A*:
 - expansion ratio = 1.07
 - dimension of the first element at the wall = $2 \cdot 10^{-7} m$
 - thickness = $0.0025 m$
- Structured part *B*:
 - expansion ratio = 1.15

- dimension of the first element at the wall = $5 \cdot 10^{-7} m$
- thickness = $0.003m$

If we use the structured part A we are able to have $Y^+ \approx 1$ while with the structured part B we reach a maximum value of $Y^+ \approx 2.2$. In both case the value of Y^+ is enough to guarantee a good resolution of the boundary layer.

Also in this case we have to set the value of h and the mesh algorithm for the unstructured part is *Delaunay*. The following table shows the meshes used during our simulations.

	h	Structured part	Elements
Mesh 1	0.0005	<i>A</i>	19892
Mesh 2	0.0002	<i>A</i>	67840
Mesh 3	0.00012	<i>A</i>	146723
Mesh 4	0.0001	<i>A</i>	196685
Mesh 5	0.0005	<i>B</i>	12002
Mesh 6	0.0004	<i>B</i>	16356
Mesh 7	0.0003	<i>B</i>	25296
Mesh 8	0.00025	<i>B</i>	33431
Mesh 9	0.0002	<i>B</i>	47738
Mesh 10	0.00015	<i>B</i>	77045

4.3 Numerical schemes

- **EULER SIMULATIONS:** In this case we consider the inviscid problem directly solving the Euler equations, without, of course, any turbulent model. To initialize the flow, we impose an almost zero Mach number (10^{-9}) and we use thermodynamic conditions for the flow specification, setting the value of static pressure and temperature. Moreover we are working with a fluid which is non ideal, but we set in any case "IDEAL_GAS" for the fluid model specifying the value of the ratio of specific heats $\gamma = 1.01767$ and the specific gas constant $R = 35.17 J/kg \cdot K$. We use the Sutherland model to compute the viscosity from the temperature.

We use Green-Gauss method to compute gradients when we use the MUSCL approximation. The value of the CFL is changed depending on the situation: when the simulation is easy to converge we use an adaptive CFL starting from a number of 10, but when it becomes harder to converge we decrease it to 1. In order to run second order simulations we activate the MUSCL_FLOW option, setting a VENKATAKRISHNAN_WANG slope limiter of 0.08 when we use the ROE scheme. During the report

we will use also the JST scheme with the second order extrapolation in order to compare the result, but the main results are presented with ROE.

For the convergence we check the residual of the density up to a value of -10 in logarithmic scale.

- **RANS SIMULATIONS:** Most of the options remains basically the same of the previous case, therefore we will present only what changes. Of course we have to change the solver and introduce a turbulence model. In particular we set the Spalart-Allmaras model for most of our simulations, but we will also try to use the SST model in order to compare the results.

Also in this case VENKATAKRISHNAN_WANG slope limiter is used with a value that is equal to 0.005 when the MUSCL option is activated.

The method is ROE and the convergence criteria is the same as before.

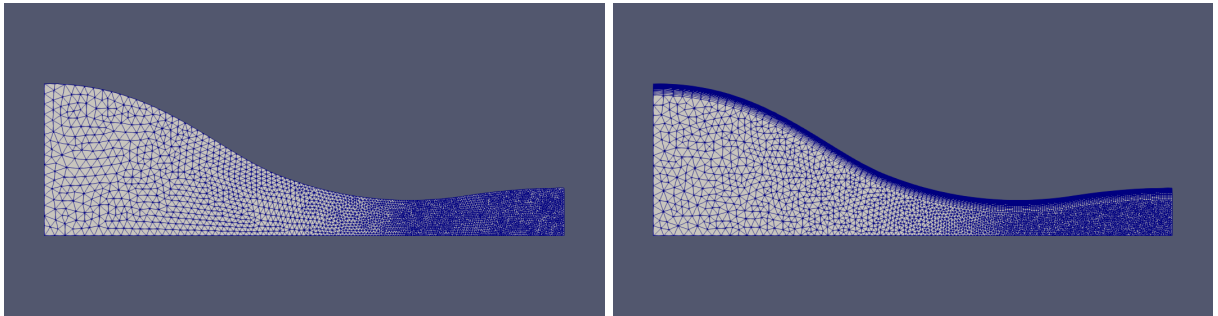


Figure 4.2: On the left: structured mesh for Euler case - On the right: hybrid mesh for RANS case

5. Results

5.1 Euler case

5.1.1 Grid convergence For all required cases, e.g. the most demanding ones

As we have already explained, the first step is to reach mesh convergence and this is done using a ROE scheme and refining the mesh both for the first and the second order (activating the MUSCL_FLOW option). In this way we are able to reach a mesh that allows us to present result which are independent from further refinements of the grid both for the first and the second order. Mesh convergence is presented for the most troublesome condition, meaning the case for which a shock wave is generated in the divergent part of the nozzle. This is obtained by imposing a pressure of 650000 Pa at the outlet as boundary condition. When we reach convergence under this condition we can say that also the subsonic and the design solutions will be independent from further refinement of the mesh.

The following figure shows mesh convergence for the Euler case for fist order ROE comparing pressure along the centerline of the nozzle. Analogous considerations can be done looking at the Mach plot. As we can notice, grid convergence is evident and with the last two meshes we obtain very similar results.

Comparison:

what and where

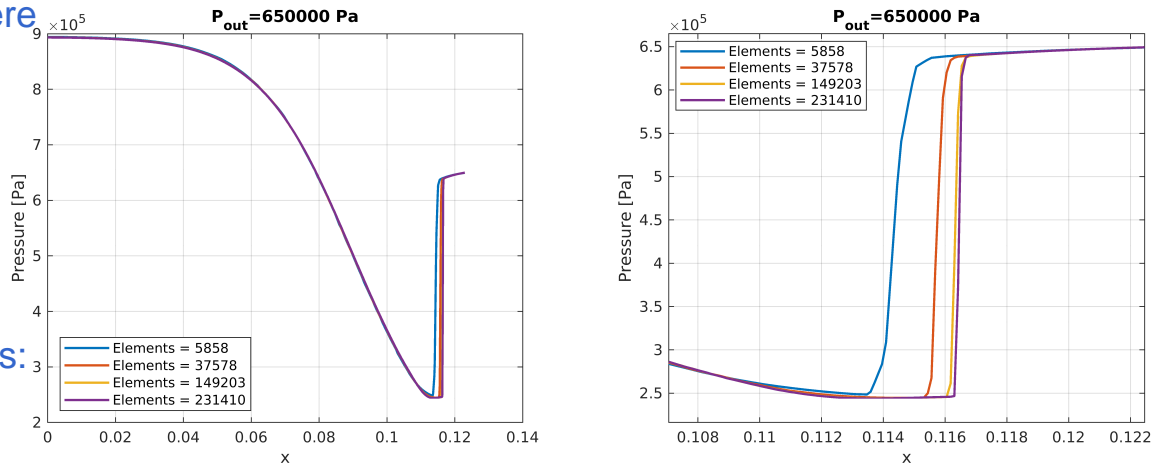


Figure 5.1: Grid convergence for first order ROE. On the right, zoom on the shock wave

Moreover, we do the same for the second order ROE and of course it is important to notice at the effect of the scheme on the shock wave. In fact we have have a less smooth solution with the comparison of overshooting before and after the shock, but this unphysical behaviour is limited as we refine the mesh. The finest mesh in fact is the one that can be considered as converged and the effect of the overshooting is basically removed. In

Clear pictures:
lines,
legend,
labels,
caption

this case we report also the Mach plot in order to show that these considerations hold also if we look to this quantity.

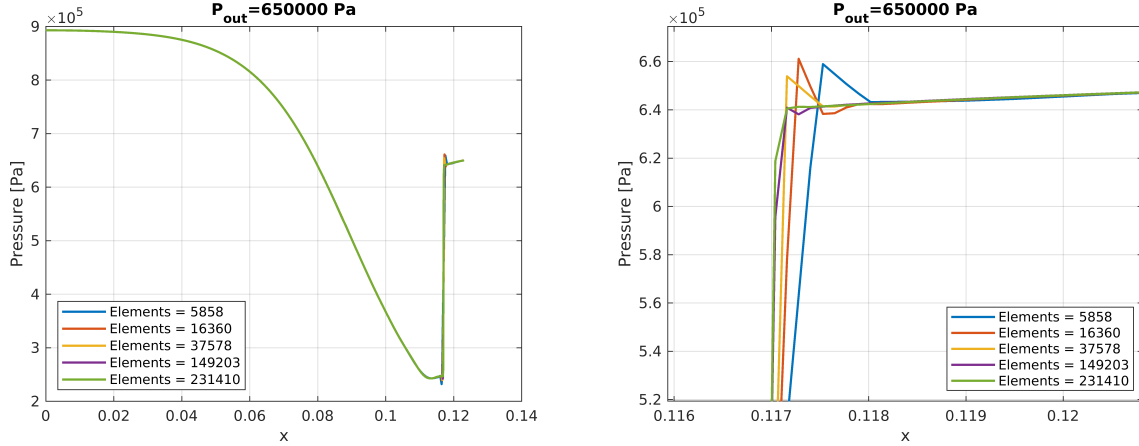


Figure 5.2: Grid convergence for second order case. On the right, zoom on the shock wave

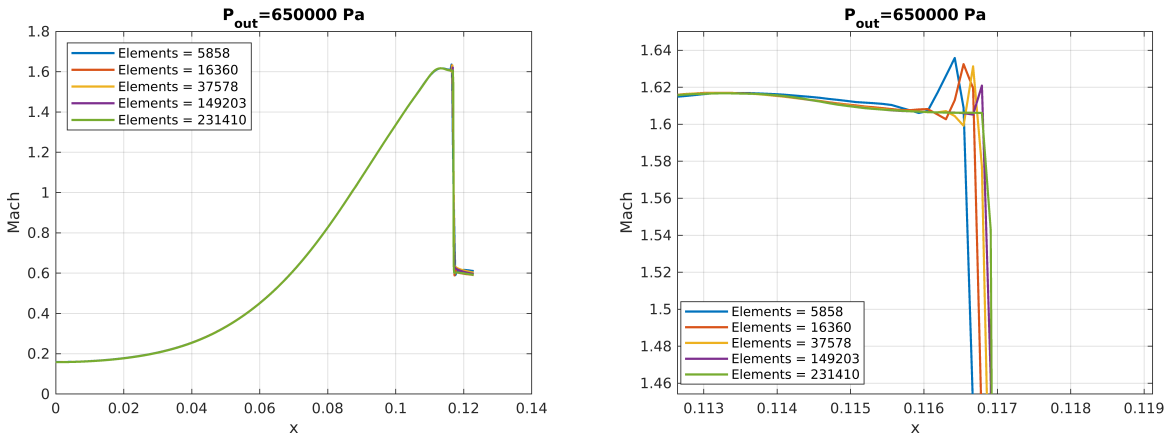


Figure 5.3: Grid convergence for second order case. On the right, zoom on the shock wave

As a consequence of this analysis the results reported in the following page for the Euler case are obtained using the finest mesh: *Mesh 5*.

5.1.2 Comparison between ROE and JST scheme

For the second order case we also try to use the JST scheme, but, as we can notice from the figures below, the solutions computed for the shock wave in the divergent condition are basically the same. However with JST scheme each simulation seems to reach convergence more easily with respect to ROE. Of course the solutions presented below are computed using the same mesh (*Mesh 4*).

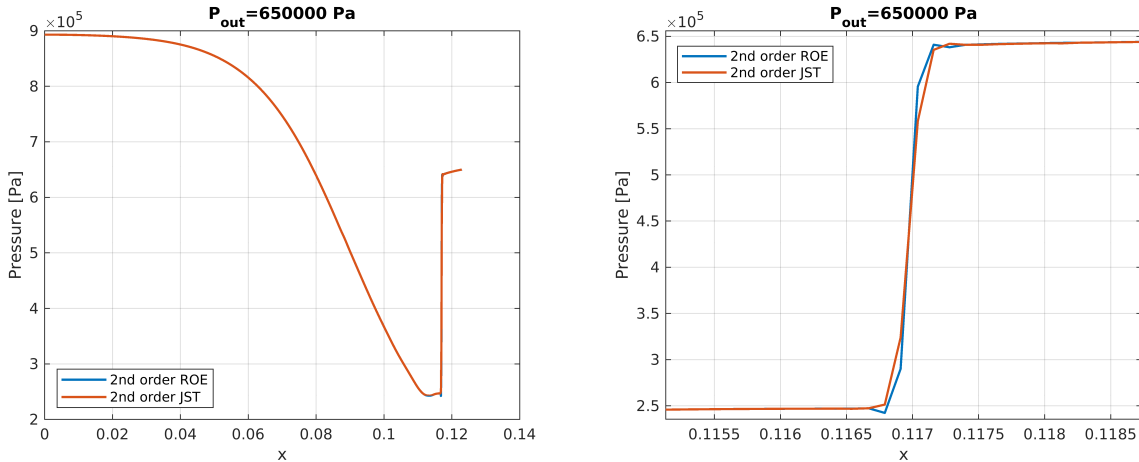


Figure 5.4: Comparison between JST and ROE solutions on the pressure. On the right, zoom on the shock wave

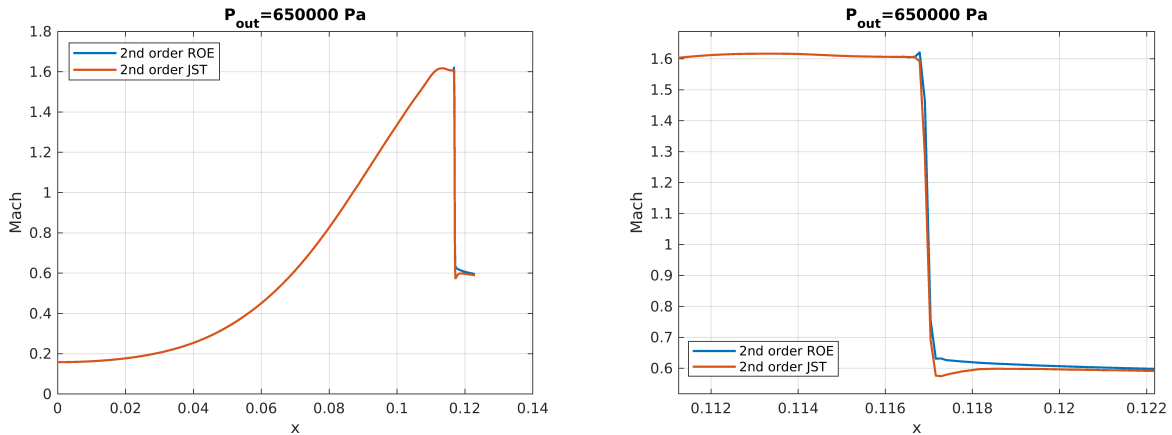


Figure 5.5: Comparison between JST and ROE solutions on the Mach. On the right, zoom on the shock wave

What we can notice is that the solutions are quite similar in most of the nozzle and they differ just a bit in the zone of the shock wave. For example for the pressure we can say that ROE scheme seems to introduce a bit more oscillation in the solution, but it leads to a steeper discontinuity. For the Mach, instead, the JST scheme causes a non physical overshooting after the shock wave while the ROE scheme solution has a small one before the shock. In any case all the following results are obtained using the ROE scheme with second order extrapolation.

5.1.3 Comparison between 1st and 2nd order solutions

In this section we compare the results obtained using first order ROE with the ones obtained with the second order extrapolation. In particular we take into account three different work conditions of the nozzle depend on the value of the outlet pressure: shock wave in the divergent $P_{out} = 650000 Pa$, design condition $P_{out} = 200000 Pa$, subsonic $P_{out} = 800000 Pa$

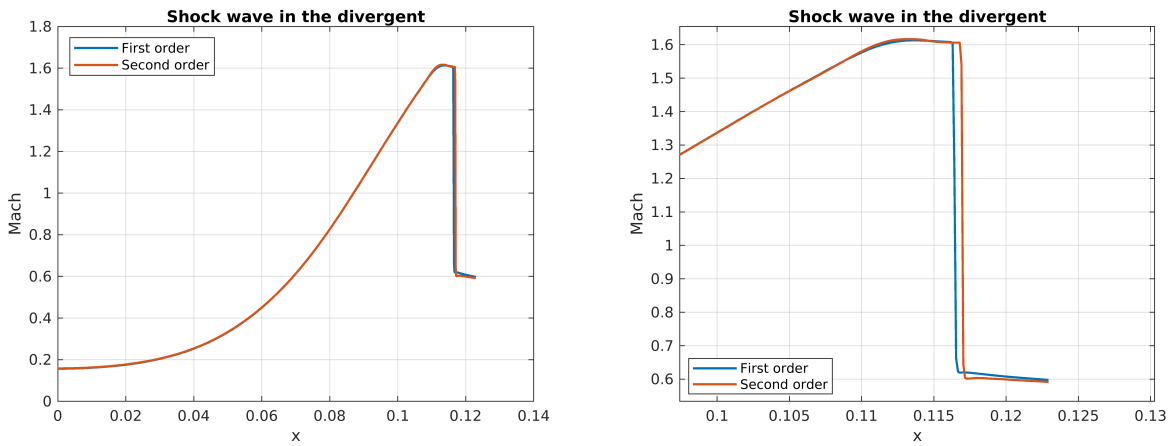


Figure 5.6: Comparison between JST and ROE solutions on the Mach. On the right, zoom on the shock wave

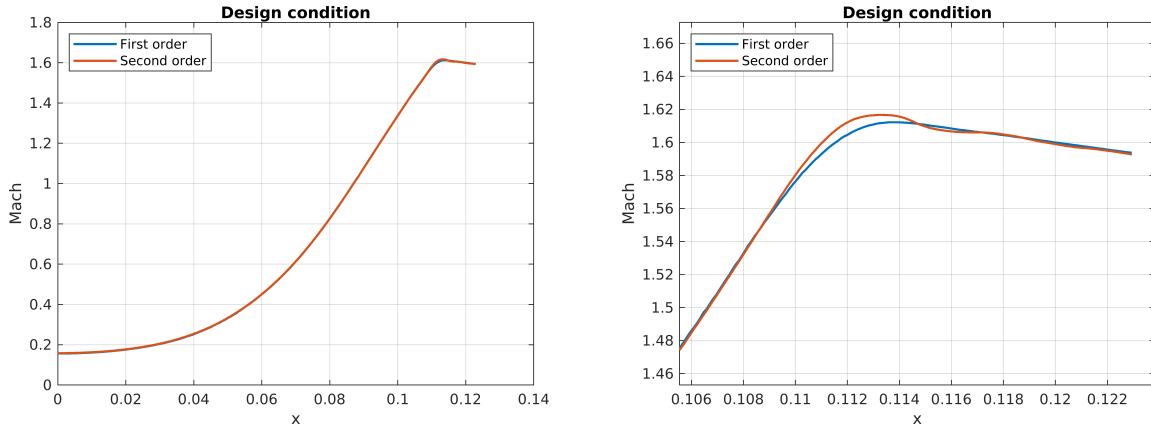


Figure 5.7: Design condition: comparison between JST and ROE solutions on the Mach

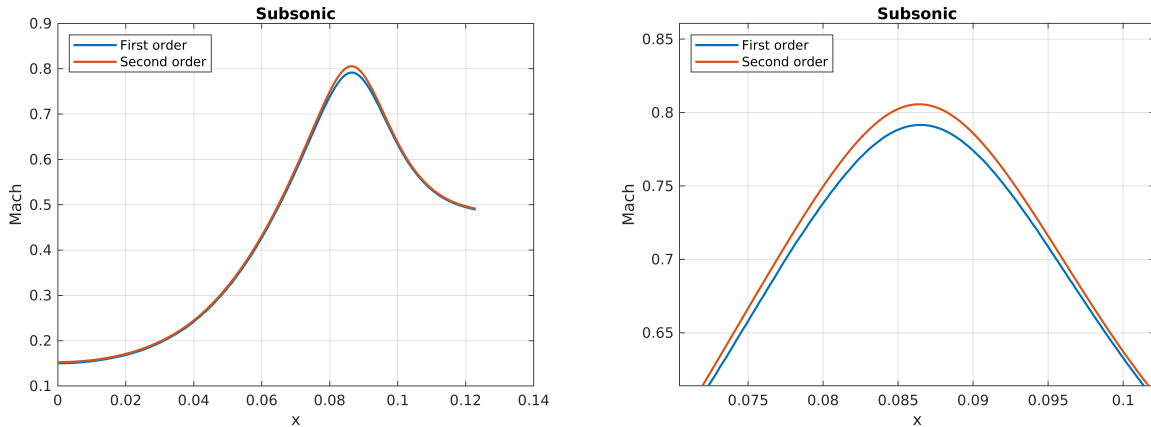


Figure 5.8: Subsonic case: comparison between JST and ROE solutions on the Mach

The second order allows us to reach more accurate results that are slightly different from the one obtained with the first order ROE. Of course one of the problem is the introduction of a bit of oscillation in the solution that are more evident in the shock wave case and in the design condition, but luckily their effect is still minimal. In the comparison with the quasi 1D theory and with the RANS case, second order solutions will be considered.

5.2 RANS case

5.2.1 Grid convergence For all required cases, e.g. the most demanding ones

Also in this case the first step consists in reaching grid convergence with a series of mesh refinements. In particular, as we have already shown in the *Mesh generation* section, setting one of the two set of parameters for the structured part, then we refine the mesh acting on the value of h . The following plots show convergence for the first and the second order method. Moreover, for the latter, we have also shown that the grid convergence obtained for the case with the shock wave in the divergent is also valid for the other two cases: subsonic and design condition.

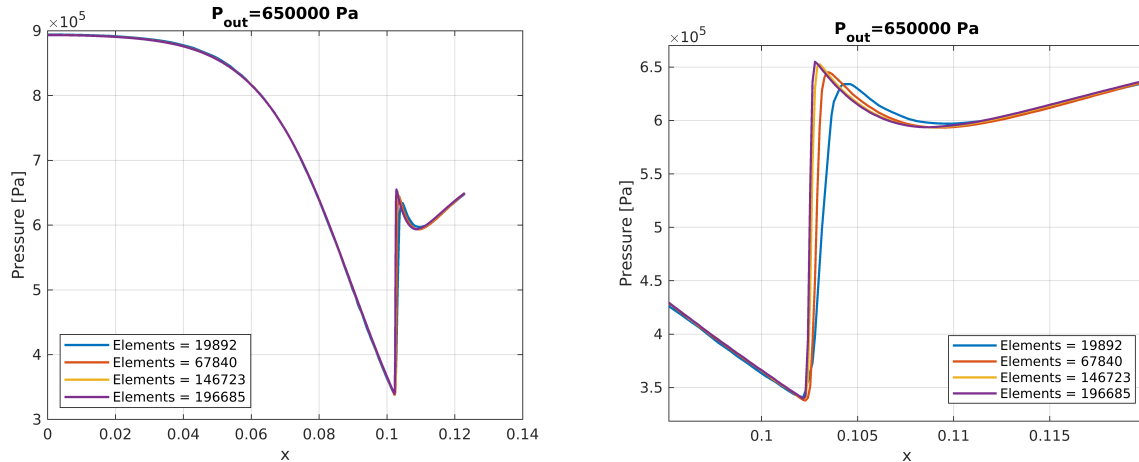


Figure 5.9: Grid convergence for first order case. On the right, zoom of the shock wave

As we can notice, for the first order ROE scheme the two finest meshes are essentially overlapped meaning that we have reached grid convergence. In this case we reach convergence after a very high refinement of the mesh, instead, as we can see from the following plots, for the second order we are able to reach convergence with a less number of elements. Moreover, as we increase the discretization the convergence of a second order simulation becomes harder. However, in the following figure is evident that grid convergence is reached with the mesh made with 47738 elements in the case with the shock wave in the divergent. After that we demonstrated also that this mesh is good also for the other two conditions since a further refinement does not lead to a big change in the results.

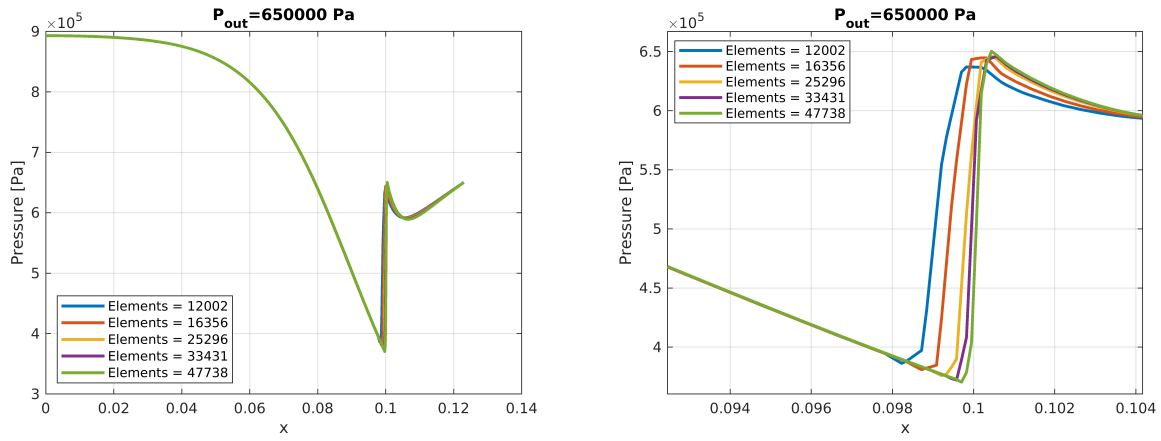


Figure 5.10: Shock wave in the divergent case: grid convergence for second order case

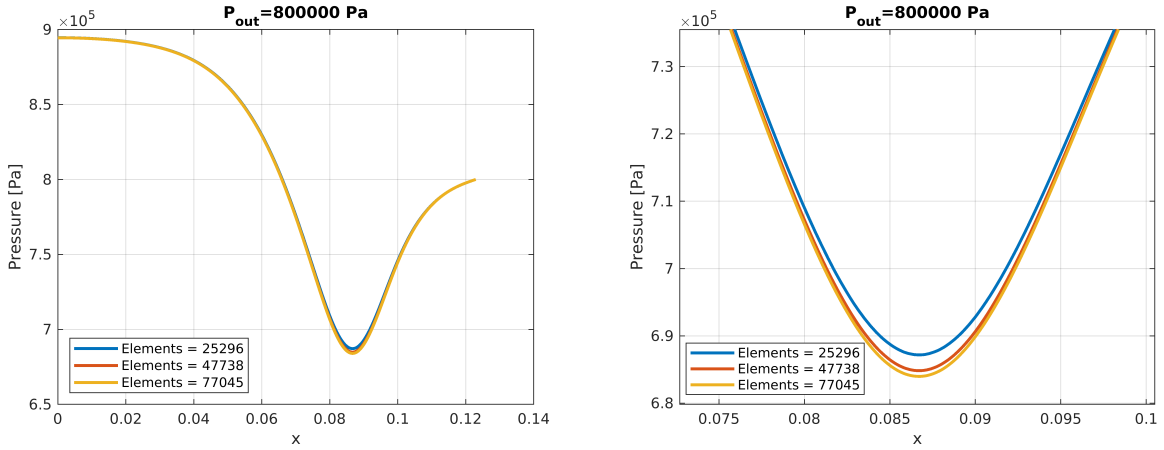


Figure 5.11: Subsonic case: grid convergence for second order case

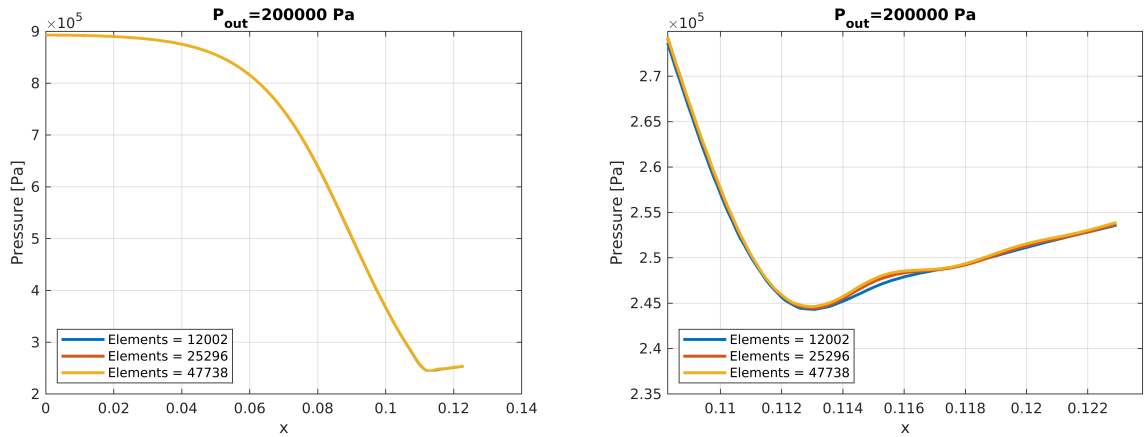


Figure 5.12: Design condition: grid convergence for second order case

5.2.2 Comparison between SA and SST turbulence model

Previous results are obtained using Spalart-Allmaras turbulence model, therefore in this section we compare this results with the ones obtained with the SST turbulence model. We have noticed that the results are almost overlapped therefore we report only the case with the shock in the divergent in which a slight difference can be notice if we zoom on the shock wave.

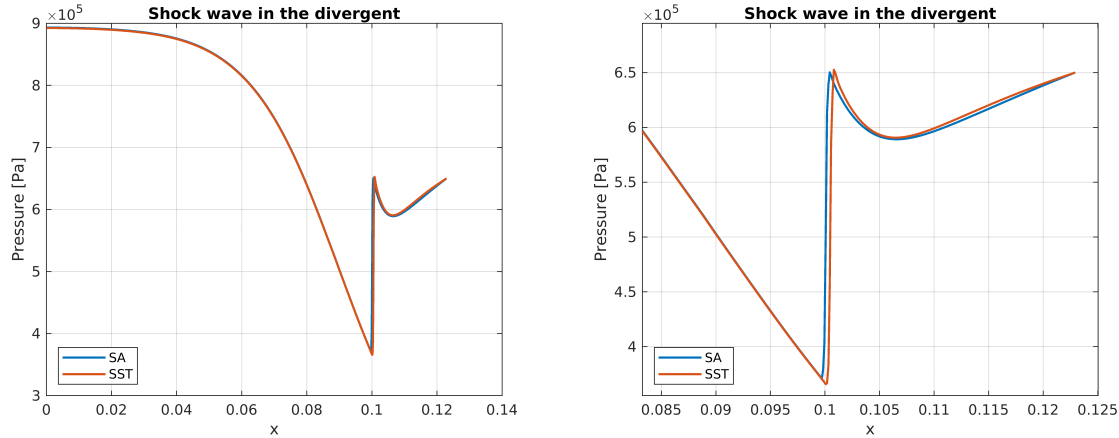


Figure 5.13: Comparison between SA and SST turbulence model

5.2.3 Comparison between 1st and 2nd order scheme

As we did for the Euler case, we compare the results obtained with the first order ROE scheme and with the second order extrapolation. The effect is basically the same that we have seen in the Euler case, therefore we do not report the plots for the subsonic case and for the design condition since the graphs are very similar to the ones already presented. On the other hand it is interesting to notice the effect of the second order on the solution with the shock wave in the divergent. The shape of the curve remains essentially the same but the position of the shock wave is a bit different. In particular the shock occurs 2mm before with respect the one obtained with the first order scheme and the jump is a bit smaller, meaning that the difference between for example the pressure before and after the shock wave is slightly smaller.

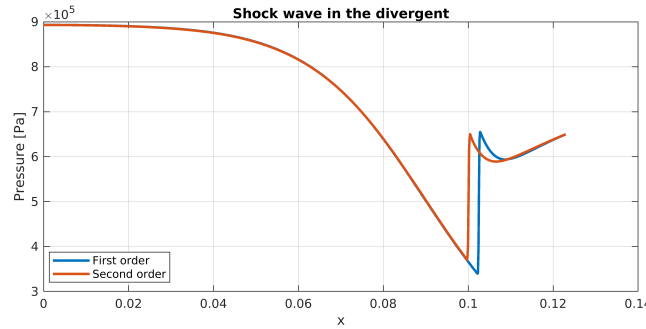


Figure 5.14: Comparison between 1st and 2nd order scheme

5.3 Comparison between Euler, RANS and Quasi 1D

The following figures shows a comparison between the results obtained for the Euler and the RANS cases for the three considered conditions of P_{out} . In the plots is reported also the solution computed using *Quasi 1D* theory. As we can notice, the results obtained for Euler and RANS cases are very different when we consider the subsonic case or the one with the shock in the divergent. Instead the solutions for the design condition are essentially overlapped. With respect to the quasi 1D theory, the Euler results are obviously closer to it since they consider the inviscid simulation as in the hypothesis of the theory. On the other hand the in the RANS case, we obtain very different solution due to the fact that we take into account also the boundary layer. In any case, the results of quasi 1D theory are not perfectly reproduced by the Euler simulations since the quasi 1D theory is based on the strong hypothesis that the flow is 1D and goes only in the direction parallel to the nozzle axis while of course it is not like this due to the nozzle shape.

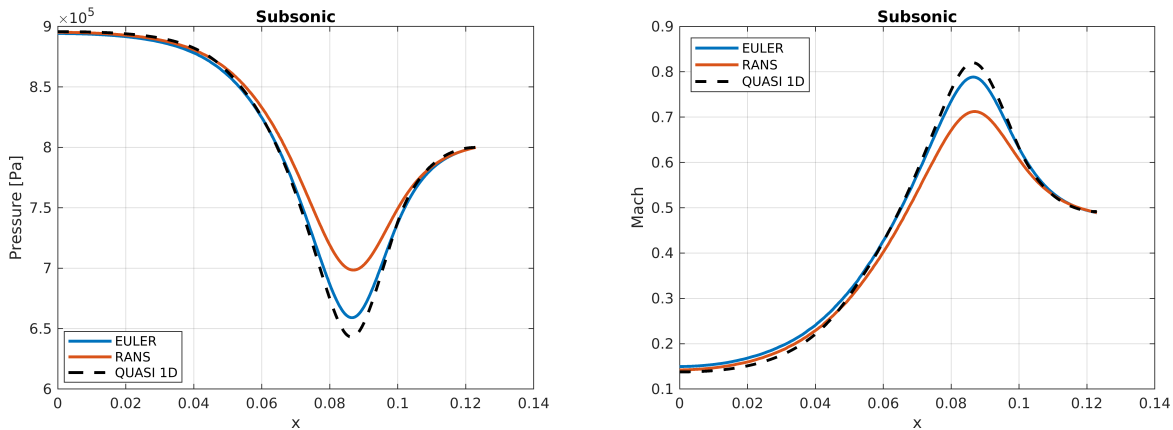


Figure 5.15: Subsonic case: comparison between Euler, RANS and Quasi 1D

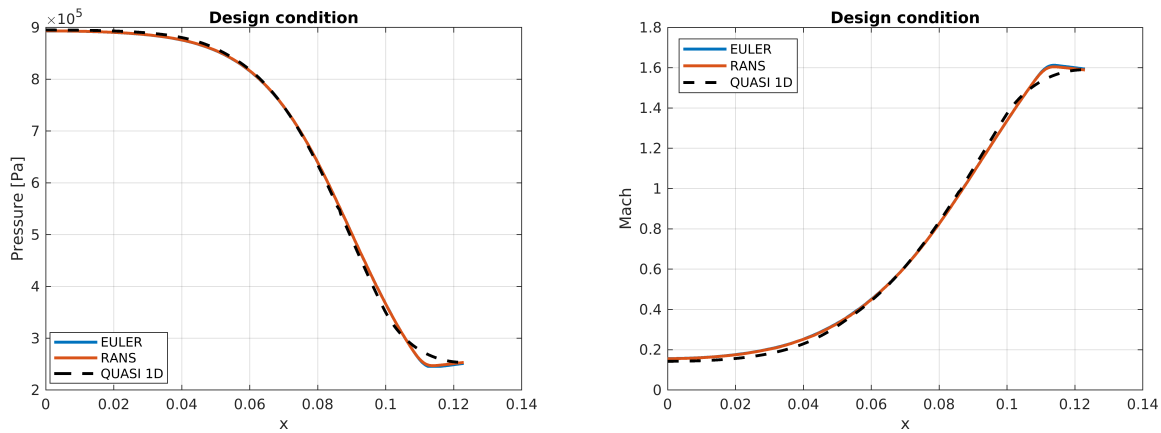


Figure 5.16: Design condition: comparison between Euler, RANS and Quasi 1D

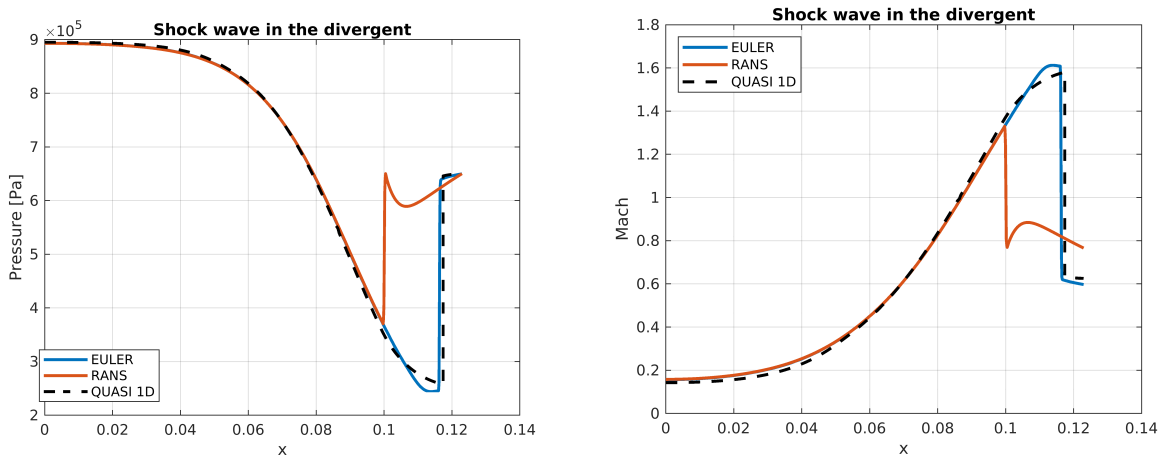


Figure 5.17: Shock wave in the divergent case: comparison between Euler, RANS and Quasi 1D

As we can notice one of the most evident difference is that when the shock wave is in the divergent, the shock occurs much sooner in the RANS case with respect to the Euler case. Moreover, in the Euler case the shock wave in the divergent is almost normal to the flow, while in the RANS case it is not straight as we can see in the following figures.

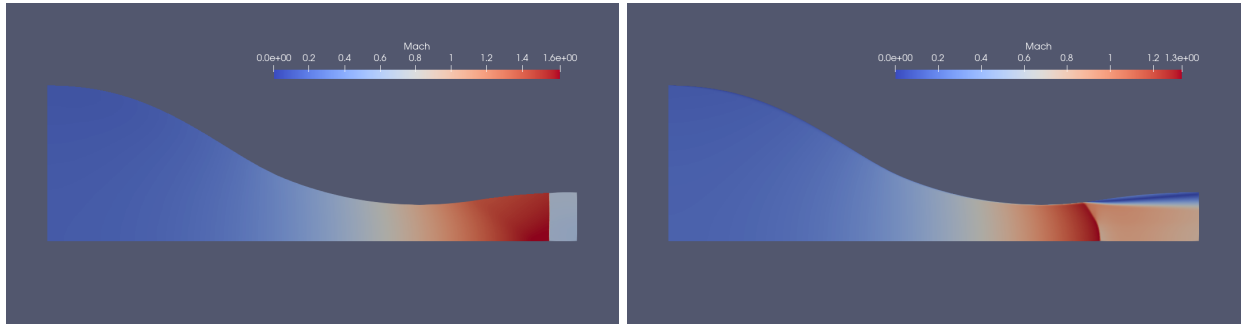


Figure 5.18: Shock wave in the divergent case: comparison between Euler and RANS

In the RANS case, we can notice also that after the shock wave, even if we have a subsonic Mach and we are in the divergent, there is a small expansion before the expected compression. This is evident in *Figure 5.16* and the explanation is linked to the formation of the separation bubble that can be noticed in *Figure 5.17*. In fact, due to the shock wave and the geometry we have a strong pressure gradient and this leads to the separation and the formation of a recirculating bubble with the effect of choking the flow and as a consequence an increase in the velocity and a decrease in the pressure.

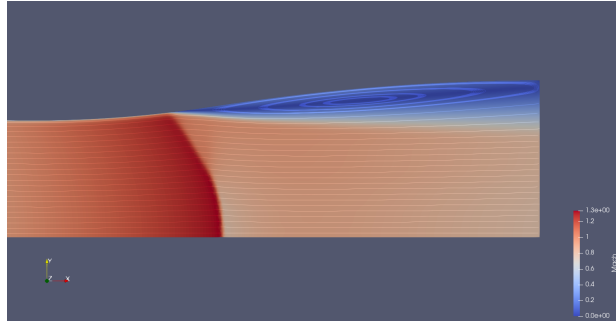


Figure 5.19: Recirculating bubble after the shock wave

5.4 Comparison with experimental data

If you use data from the literature, cite the references

In this section we compare the obtained results for the design condition with the experimental data reported by *Spinelli A., Cammi G., Gallarini S., Zocca M., Cozzi F., Gaetani P., Dossena V., Guardone A.* Experimental evidence of non ideal compressible effects in expanding flow of a high molecular complexity vapor, *Experiments in Fluids* (2018) 59:126. We have noticed that, we are able to reproduce these data if we modify some setting of our .cfg file that provides a better description of the fluid. In particular, instead of setting *IDEAL_GAS* as fluid model we set *PR_GAS* and, therefore, in addition to the value of γ and of the gas constant, we have to indicate also the value of: critical temperature, critical pressure and acentric factor. Moreover, instead of Sutherland model for viscosity we assume constant viscosity and then we also introduce *CONSTANT_CONDUCTIVITY* as thermal conductivity model. The boundary conditions remain the same as before, but for the inlet and outlet we set them using *MARKER_RIEMANN*. All the other settings remains the same, therefore we use ROE scheme with second order extrapolation and SA turbulence model. In this way, using our converged meshes we obtain the following solutions that reproduce the experimental data.

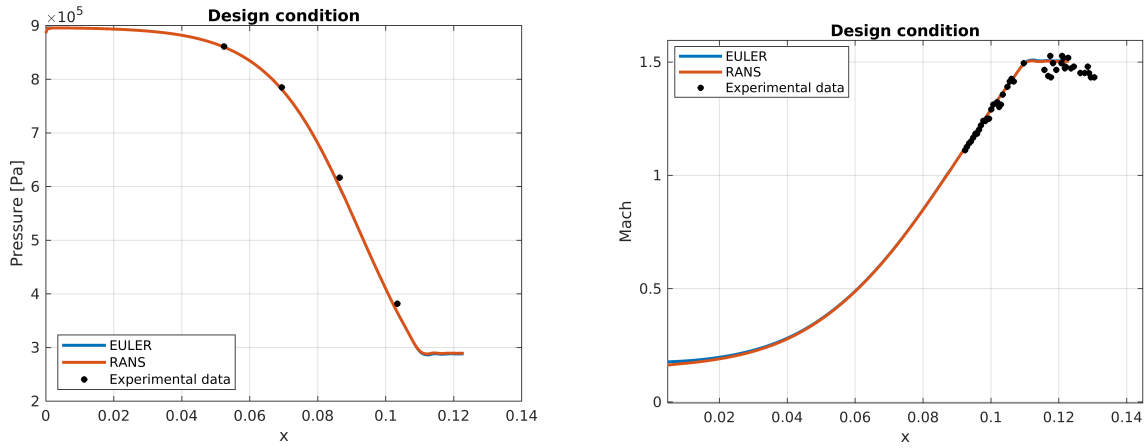


Figure 5.20: Comparison with experimental data

5.5 Sauer method

As we have explained in the theoretical part in order to apply the Sauer method we need essentially two parameters: curvature radius r_t and throat height y_t . Moreover, for the hypothesis to be valid $r_t/y_t > 2$. For our case the value of y_t is known while the curvature radius can be estimated. In particular we choose $r_t = 10 \cdot y_t$ so that we can apply the method and find the sonic line. the following figures show a comparison between the sonic line obtained with our numerical simulations and the one computed with the Sauer method. As we can see, with the choice made for the curvature radius, the two sonic line have basically the same shape. For the comparison design condition of the nozzle has been considered.



Figure 5.21: RANS case: comparison between numerical results and Sauer method

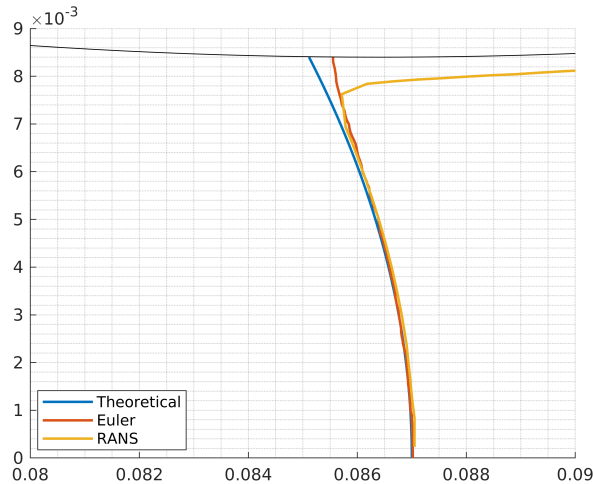


Figure 5.22: Sonic line comparison between numerical results and Sauer method

6. Conclusions

The analysis of the flow inside the nozzle with Euler and RANS solver leads us to some considerations. We have noticed that the results obtained in the two cases are very similar if the nozzle is in design condition while they are a bit different in the subsonic case. In this last case in fact, the presence of boundary layer leads to a less pronounced expansion in the convergent and a compression in the divergent. However the most evident differences can be appreciate in the case with the shock wave in the divergent. In particular, the shape and the position of the the shock wave is totally changed: the shock occurs much sooner in the RANS case with respect to the Euler case and in Euler case the shock wave in the divergent is almost normal to the flow, while in RANS case it is curved. Moreover, in RANS case, we can notice also that, due to the shock wave, we have a strong pressure gradient and this leads to separation and the formation of a recirculating bubble. With respect to the *Quasi 1D* theory we can say that the Euler case is much closer to its prediction. This is due the fact that in Euler simulation we consider inviscid conditions as in *Quasi 1D* hypothesis. In any case, the results of quasi 1D theory are not perfectly reproduced by the Euler simulations since the quasi 1D theory is based on the strong hypothesis that the flow is 1D and goes only in the direction parallel to the nozzle axis while of course it is not like this due to the nozzle shape.